LDD Land Degradation & Development

A case study on history and rates of gully erosion in Northeast China

Journal:	*Land Degradation & Development*
Manuscript ID	LDD-21-0077.R1
Wiley - Manuscript type:	Research Article
Date Submitted by the Author:	06-May-2021
Complete List of Authors:	WEN, Yanru; Chinese Academy of Agricultural Sciences Institute of Agricultural Resources and Regional Planning, Soil Health Care; Northeast Institute of Geography and Agroecology Chinese Academy of Sciences, Soil Heal Care Kasielke, Till; Ruhr University Bochum, Geographical Institute Li, Hao; Northeast Institute of Geography and Agroecology Chinese Academy of Sciences, Soil Heal Care Zepp, Harald; Ruhr University Bochum, Geographical Institute Zhang, Bin; Chinese Academy of Agricultural Sciences Institute of Agricultural Resources and Regional Planning, Soil Health Conservation
Keywords:	Gully erosion, Erosion rate, Remote sensing, 137Cs, Mollisol

SCHOLARONE™
Manuscripts

Graphical abstract

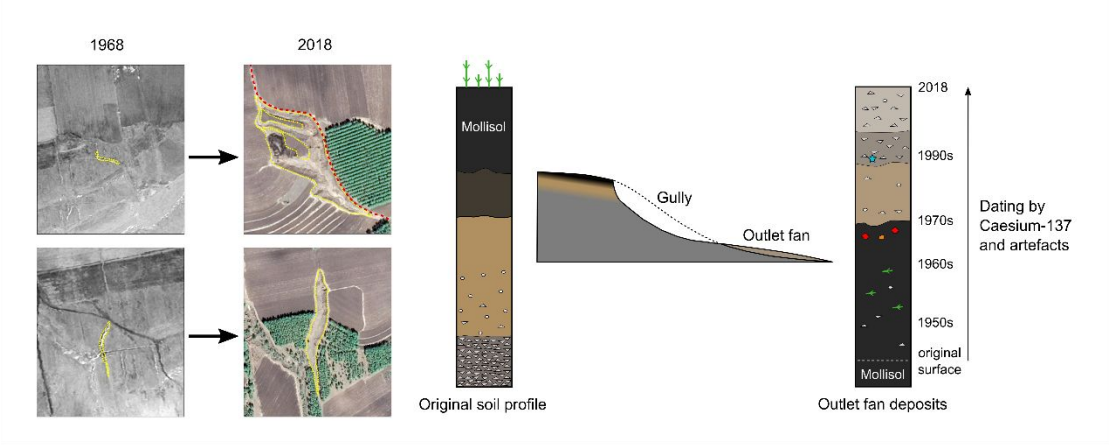

For Peer Review

Highlights

- Gully initiation years were estimated from morphology change and ^{137}Cs dating.
- Gully volumes were measured to estimate soil loss using unmanned aerial vehicle.
- Gullies were mostly initiated in the 1950s to 1960s due to large-scale agricultural expansion.
- Gully heads retreated at 1.5 to 2.5 m yr^{-1} and soil loss at 25.7 to 44.7 Mg yr^{-1} ha^{-1}

For Peer Review

A case study on history and rates of gully erosion in Northeast China

Yanru Wen[1,2], Till Kasielke[3], Hao Li[4], Harald Zepp[3], Bin Zhang[1]*

[1] Institute of Agricultural Resources and Regional Planning, Chinese Academy of Agricultural Sciences, Beijing, 100081, PR China.

[2] Key Laboratory of Agricultural Remote Sensing (AGRIRS), Beijing, 100081, PR China.

[3] Department of Geography, Ruhr-University Bochum, Universitätsstr.150, 44780 Bochum, Germany.

[4] Northeast Institute of Geography and Agroecology, Chinese Academy of Sciences, Harbin, 150081, PR China.

*Corresponding author:

B Zhang, E-mail: zhangbin01@caas.cn. Tel/Fax: +86 10 82105635

Manuscript submitted to: Land Degradation & Development

Submission date: 4 February, 2021

For Peer Review

Abstract

Mollisols are of major importance for food security worldwide but are increasingly degraded by soil erosion. Mollisols in Northeast China have been converted into agricultural use only since the 19th century, but gullies are widely distributed. Gully erosion history, rates and causes in this region remained unclear. We chose a study area with landforms and land-use history typical for the central Mollisol region of Northeast China to estimate the initiation years and rates of gully erosion from 1968 to 2018 by using aerial and satellite imageries. The outlet fan deposits of a large gully system were dated by Caesium-137 (^{137}Cs) and artefacts. Local farmers were interviewed to verify the results. Gully volumes were measured by structure-from-motion technique using photos taken from an unmanned aerial vehicle. Our results showed that gully systems had already appeared on the steep slopes and along unpaved roads in 1968. They had become larger and more complex in 2018 by upslope retreat of the main gullies and side gully formation. Gully incision started in the 1950s and 1960s, when the original grassland and forest were completely converted into arable land. From 1968 to 2018, the gully density increased from 1.2 to 2.3 km km^{-2} and the gully heads retreated at speeds from 1.5 to 2.5 m yr^{-1}. The soil loss from gully erosion ranged from 25.7 to 44.7 Mg yr^{-1} ha^{-1}. These data demonstrate the severity of gully erosion in the Mollisol region of Northeast China and underline the importance of appropriate countermeasures.

Keywords: Gully erosion; Erosion rates; Remote sensing; Caesium-137 ^{137}Cs; Radioisotope dating; Northeast China

For Peer Review

1. Introduction

Mollisols cover ~7% of the global ice-free land area. They are the most important soil order for food production because of their deep surface horizons with a high content of soil organic carbon. Mollisols are severely threatened by soil degradation under practiced soil management as they have globally been converted from native forest and grassland into arable lands since the 19th century (Liu et al., 2012). In Northeast China, Mollisols have been used for agriculture on a large scale since the 1950s (Ye & Fang, 2011). The Mollisol region has become the largest granary in China since the late 1990s, contributing to the annual food demand of more than 216 million urban citizens (Liu et al., 2011). More than 290,000 active gullies longer than 100 m exist in the Mollisol region (Ministry of Water Resources, 2010), posing one of the biggest threats to local soil quality and national food security (Liu & Yan, 2009).

Studies from around the world show that gully erosion has occurred in different periods of history (Dotterweich et al., 2003; Dotterweich, 2013; Dreibrodt et al., 2010; Mieth & Bork, 2010). In central Europe, for instance, gully erosion in medieval and modern times was caused by the combination of land use and extreme rainfall events (Dotterweich, 2008). More recently, gully erosion has become a widespread and more permanent problem in many parts of the world. Land-use change, especially forest clearance for agricultural activities, was identified as a main driver of gully erosion (Castillo & Gomez, 2016). In Northeast China, soil erosion problems have occurred since arable land expanded and agriculture was intensified during the 1950s (Ministry of Water Resources et al., 2010). However, the onset of gully erosion in the Mollisol region is still unclear.

Gully erosion rates may vary considerably between and within the regions, depending on environmental conditions, catchment drainage size and gully dimensions

For Peer Review

(Castillo & Gomez, 2016; Poesen et al., 2003; Xu et al., 2019a). Previous research in the Mollisol region has studied erosion rates of a single gully (An et al., 2014) or monitored short-term gully head retreat and erosion rates of ephemeral or small permanent gullies (Hu et al. 2007; Wu et al., 2008; Zhang et al., 2007). Recently, Li et al. (2021) presented a study on long-term changes of gully density. Yet, little information is available on long-term erosion rates in the Mollisol region.

Gullies often develop along drainage lines on slopes, becoming larger in gully area and volume due to gully heads retreating backwards up the slope, sidewalls collapsing and downcutting (Aber et al., 2019; Harvey, 1992). Gully expansion rates are often expressed as gully head retreat distance or gully area and volume changes measured using global positioning system (GPS) or airborne photography over a defined period (Gudino-Elizondo et al., 2018; Vandekerckhove et al., 2001). However, analysis of historical aerial photography is often constrained by poor image resolution or availability. Thus, the timing of gully initiation and expansion is only roughly estimated, particularly for gullies older than about 70 years (Castillo & Gomez, 2016; Frankl et al., 2012; Marzolff & Poesen, 2009; Poesen, 2018; Tebebuet al., 2010). Therefore, local farmers' and experts' knowledge (Frankl et al., 2011; Moges & Holden, 2008; Nyssen et al., 2006) and Caesium-137 (^{137}Cs) are often used to investigate the erosion history since the 1960s (Porto & Walling, 2012; Zhang et al., 2017). Dating of colluvial deposits by embedded artefacts and other dating techniques may also give insights into soil erosion history on a local scale (Bork & Lang, 2003; Dotterweich et al., 2003; Mieth & Bork, 2010; Kappler et al., 2018; Kasielke et al., 2019; Kasielke & Zepp, 2011; Vattuone et al., 2018).

The objectives of this study were to 1) characterize gully changes over a time interval of 50 years (1968 to 2018) in an agricultural area representative of the Mollisol

For Peer Review

region in Northeast China, 2) estimate gully initiation years and erosion rates, and 3) understand the gully erosion processes and driving forces in the region.

2. Materials and Methods

2.1. Study area

Our study area (20 km²) is located in Guangrong village, about 15 km southwest of Hailun city (Heilongjing Province of China) in the central part of the Mollisol region of Northeast China (Fig. 1). This region has a temperate continental monsoon climate. The mean annual temperature is 1.5 ℃, with the highest mean monthly temperature of 21.7 ºC in July and lowest in January (-21.8 ℃). The frost season lasts from late October to late April. The mean annual precipitation is 543 mm, about 78% of which is distributed from June to September. Over the last 58 years, since a weather station was established, there were 32 storm events with a rainfall intensity > 50 mm d^{-1} and two with recorded rainfall as high as 85.3 and 112.7 mm d^{-1} in June of 1966 and 1975, respectively.

The regional soils were classified as Typic Hapludoll according to the USDA Soil Taxonomy System (Soil Survey Staff, 2010), corresponding to Haplic Phaeozem in the FAO classification (FAO, 2015). The mollic epipedon was up to 70 cm in depth and developed in Pleistocene loess with a high clay content of 35 to 45 % (Sui et al., 2013; Qiao et al., 2015), which was underlain by fluvial sediments of varying grain size (silt, sand, pebbles) and shale (Sun & Liu, 2001).

The study area is typical for the Mollisol region regarding landforms and land-use history. The slopes are long (> 200 m) and gentle (< 5%). Gullies account for 3.2% of the administrative village area and gully density is 2.4 km km^{-2}, which is typical for the Mollisol region (Li et al., 2016). Land reclamation in the Guangrong village was started

For Peer Review

in 1896 by several migrant families. Today, arable land accounts for 80% of the study area.

2.2. Gully change between 1968 and 2018

The earliest available aerial photograph from 16th September 1968 and a satellite image from 19th July 2017 were collected for the studied area. The aerial photograph was available from the Heilongjiang (Province) Bureau of Surveying and Mapping Geographic Information, with a scale of 1:15,000 and a resolution of 0.6 m. The satellite image was available from the Digital Globe of Google, with a resolution of 0.3 m. These images were geo-referenced in a GIS environment using the UTM 52N coordinate system. A Digital Elevation Model (DEM) of the study area was created by digitizing the contour lines from a topographical map from 1982 (scale 1:10,000) and subsequent interpolation. The DEM of the study area was automatically divided into 20 catchments using the Hydro-Tool in GIS, with some adjacent small drainage areas being manually merged into Catchments No. 2, 8 and 14 (Fig. 1c). The longest gully that connected the outlet and the uppermost gully head was defined as the main gully in each catchment. Based on the aerial photo from 1968 and the satellite image from 2017, we mapped forest as areal features and cart roads and gully systems as line features (Fig. 1). The detected gullies were carefully checked in the field using differential GPS (Galaxy G6 RTK system, South Surveying) in early April 2018. Therefore, the gullies detected in the 2017 satellite image are reported as from 2018. During field mapping, the gullies

For Peer Review

without vegetation cover on the gully walls or with fresh sediments on the gully floor were marked as active gullies. All other gullies were marked as inactive.

The boundaries of the four gullies A-D in 1968 were mapped according to the gully edges visible in the aerial photo. All these 1968 gullies lie within the extended gully area from 2018. We determined total gully length by measuring the lengths of all gullies including their side gullies for 1968 and 2018. If a catchment included several independent gullies, we took only the longest gully in 2018 to measure the main gully length. However, all gullies of a catchment were considered when measuring total and active gully length. The gully density of each catchment was calculated as the total gully length divided by the catchment area.

2.3 Measurements of gully volume and erosion rates

Gullies A–D (Fig. 1), which had already appeared on the aerial photo of 1968, were used to determine gully area, gully volume and rates of gully head retreat. Gully volume was measured in April 2018 by structure-from-motion with multi-view stereo photogrammetry (SfM-MVS) using photos taken by an unmanned aerial vehicle (UAV) (DJI Phantom 4, Shen Zhen DJI Technology Co., Ltd). At that time, the gully floors were neither covered by snow nor by growing plants so that there was a minimum impact of vegetation. The digital camera captured one image per second from 50 m above the ground and was mounted facing 15% from vertical to avoid doming deformations. SfM-MVS techniques were used to create a Digital Surface Model (DSM) and an orthophoto of the targeted gully system from a series of non-calibrated

For Peer Review

images. 6-8 ground control points (GCPs) were located in the places without vegetation within Gullies A-D and in their surroundings (Fig. S1). Elevation and position of the GCPs were measured using a differential GPS with a vertical accuracy of 8 mm. The DSM with a 0.3 m spatial resolution and the orthophoto with a 0.04 m spatial resolution were generated using Pix4D mapper software (Pix4d, Lausanne, Switzerland) and geo-referenced using ArcGIS software. During the process, at least 4 GCPs were manually located in all the images to create the dense 3D point cloud and the remaining GCPs were used as checkpoints for self-calibration based on average root-mean-square error (RMSE). The best DSM was created when RMSE of the surface height of the calibrated GCPs was less than 0.010 m. The processing and camera self-calibration results are shown in Table S1.

The gully boundaries were estimated using the DSM and the orthophoto. Within these gully boundaries, we reconstructed the original slope surface before gully incision (DEM_0) by interpolating the elevation of the boundaries. Using the cut-and-fill tool in the ArcGIS environment, the gully volume was calculated as the volumetric difference between the DEM_0 and the DSM from 2018.

We calculated the average soil loss rate per catchment area (Mg yr^{-1} ha^{-1}) according to Tebebu et al. (2010) (Eq. 1).

$$R = \frac{V * Bd}{T * A} \quad (1)$$

where, R is the yearly soil loss rate per catchment area; V is the gully volume (m^3); Bd is the average of soil bulk density (1.27 g cm^{-3}); T is the number of years covering the formation of a gully; A is the gully catchment area (ha). Soil bulk density was

For Peer Review

determined using cylinder samples taken in Oct. 2017 from depths of 0-10, 10-20, 20-40, 40-60 and 60-100 cm in three reduplications in an open pit located near the head of Gully A.

The initiation years of the selected gullies were estimated based on its area in 1968 and its expansion rate estimated between 1968 and 2018 according to Nyssen et al., 2006 (Eq. 2).

$$T_1 = T_2 - \frac{A}{R_A} \quad (2)$$

where, T_1 is the gully initiation year; T_2 is the year of 2018; A is the gully area in 1968 (m^2); R_A is the area extension rate (m^2 yr^{-1}) defined as the difference of the gully area between 1968 and 2018 divided by 50 years. The calculated initiation years were checked by interviews with local farmers.

2.4. Gully outlet fan deposits and ^{137}Cs measurement

Within a 250 m-long trench at the outlet fan of Gully A (Fig. 1c), thirteen soil profiles were described. Soil texture of each layer was estimated by finger test (texture classes according to FAO, 2006). Three profiles were sampled in 5 cm intervals to determine the vertical distribution of ^{137}Cs. In addition, an old (> 80 years) forest on a flat topography was selected as a reference site without soil erosion to measure the ^{137}Cs activity. ^{137}Cs is an artificial radionuclide (half-life: 30.2 years) produced by nuclear weapons testing (Sutherland, 1989; Walling & Quine, 1990), especially in the 1960s. Fallout ^{137}Cs is rapidly absorbed to the fine fraction of surficial soils and eventually redistributed by erosion (Owens et al. 1997). The soil samples were air-dried and passed through a 2 mm sieve for the measurement of radioisotope concentration using an ORTEC spectrometer with an HPGe detector of GWL-120-15 (AMETEL-AMT ORTEC Co.) The samples were detected at 662 keV peak with a counting time over

For Peer Review

80,000 s, providing a measurement precision of ± 5% for ^{137}Cs at the 95% confidence level (Fang et al., 2012).

3. Results

3.1. Gully development between 1968 and 2018

Most of the gully systems had already appeared in 1968 (Fig. 1). The highest gully density in both years was found where the terrain was steepest, with slopes ranging from 5% to 11% (Fig. 1c). Gullies A–C retreated to the hilltops since 1968 along unpaved field cart roads, or paths made by pedestrians and cattle (Fig. 2). Compared to 1968, the gully systems had become larger and more complex by gully head retreat, gully widening, downcutting and the development of side gullies until 2018 (Fig. 1 and Fig. 3).

The total gully length increased from 24.0 to 46.7 km and total gully density from 1.2 to 2.3 between 1968 and 2018. In 2018, the gully densities in the 20 catchments ranged from 0.9 to 6.0 km km^{-2}, with fifteen of which having a gully density ≥ 2.0 km km^{-2}. About 90% of the total gully length in 2018 was actively eroding. Even under forest, 82% of 23.5 km were active (Table 1).

3.2. Gully initiation years and erosion rates

Based on the gully dimensions in 1968 and the extension rate between 1968 and 2018, we calculated initiation years between 1955 and 1966 for the Gullies A–D, which is consistent with the onset of gully development reported by the local farmers (Table 2). The oldest and largest Gully A (Fig. 3d) had a catchment area of 43.9 ha and a volume of 93,780 m^3 in 2018, giving a mean soil loss rate in the catchment area of 42.4 Mg yr^{-1} ha^{-1}. For the other three Gullies B–D with catchment areas between 5.4 and 12.7 ha and volumes between 7,630 and 17,045 m^3 the yearly soil loss ranged from 25.7 to 44.7 Mg

For Peer Review

yr^{-1} ha^{-1}. The gully head retreat rates of the four gullies ranged from 1.5 to 2.5 m yr^{-1} and the gully area increased by 57 to 165 m^2 yr^{-1} (Table 2).

3.3 Soil profiles at the gully outlet fan

The soil profiles along the trench at the outlet fan of Gully A showed that the original mollic horizon was buried by sediments eroded in the gully at different depths (Fig. 4, Fig. 5). Profile P1 started with black silty clay at the bottom below 80 cm, turning into dark greyish brown silty clay and loam between 65 and 80 cm. A high ^{137}Cs activity was detected at a depth of 75 to 95 cm (Fig. 5). The upper 65 cm of the profile was stratified, and soil colors ranged from darker brownish grey to pale yellowish brown. At a depth of 42 cm, we found plastic material from a detergent container. Profile P2 generally resembled P1. Again, plastic material appeared at about 60 cm. We encountered some shale fragments and pebbles right on top of the black material. Profiles P3 and P4 contained brownish silty clay free of coarse fragments, underlain by black material in P4.

Profiles P5 to P13 possessed intercalated layers containing coarse fragments. In P5, in common with P7, the black material is underlain by brownish material. The upper boundaries of the two lowermost layers of P5 below the black material were inclined, which is unlikely for horizon boundaries in Mollisols. Furthermore, the second lowermost layer showed an alternation of thin layers with variable content of organic matter, proving its colluvial origin. Hence, the overlying black material was also a colluvial deposit. In the middle layer of P6, undecayed grass remains and alternating thin beds of different color indicate the colluvial nature. In profile P7 we found slag, coal, coke ash, and brick fragments between 95 and 120 cm as well as undecayed grass remains. The underlying silty clay layers contained pebbles and shale (Fig. 4). Between 75 and 115 cm ^{137}Cs could be detected in every sample and the activity partly reached

For Peer Review

high values of more than 5 Bq kg^{-1} (Fig. 5). Varying contents of coarse material occurred in the upper 60 cm and below 140 cm. Profile P8 is made up of a matrix with varying colors and full of shale fragments down to 120 cm, underlain by black silty clay. The upper parts of P9 and P10 revealed brownish laminated fines with shale fragments. In P9, lenses and laminae of pale soil within the lowermost black layer indicated its colluvial origin. The black layers in P11 and P12 were remarkably thick, being 100 and 80 cm, respectively. Profile P11 had several striking features: The greyish-black fine soil overlaid brownish silty clay with a sharp boundary, dipping from 140 to 205 cm. Both layers contained well preserved remnants of horsetail (*Equisetum*) stems, indicating a young colluvial origin. Above an intermediate layer, we found fine-layered silt loam between 75 and 92 cm. The top layers had varying textures and colors and contain shale particles (Fig. 4). Continuous ^{137}Cs activity was measured between 95 and 140 cm, with a maximum at 100 cm (Fig. 5). Profile P13 started with a black layer, exposed between 75 and 120 cm, which was overlain by a brownish-grey soil material. Above it, all layers contained shale fragments, and at a depth of 40 cm, we encountered a brick fragment (Fig. 4).

4. Discussion

4.1. Gully erosion history

The analysis of the aerial photo of 1968 (Fig. 1a) demonstrated that gully erosion was already severe in the study area in the 1960s. Based on the gully area and gully extension rate, we calculated that the gullies initiated in the mid-1950s and 1960s. There are some uncertainties related to this estimation, as we used a constant gully area expansion rate between 1968 and 2018 (Eq. 2), while gully-head incision is often a non-linear process (Castillo et al., 2016; Poesen et al., 2003). The first stage of gully initiation

For Peer Review

may comprise only about 5% of the entire gully lifetime, but in that stage more than 90% of gully length, 60% of its area and 35% of the gully's volume may be formed (Kosov et al., 1978). Thus, gully incision may have started somewhat later than calculated. However, the aerial photo of 1968 proves that the gullies already existed at that time. As the calculated years of gully initiation agree with the initiation times reported by the local farmers (Table 2) and the onset of large-scale arable farming in the study area, we conclude that the linear back-dating approach provided reliable results.

The soil profiles at the outlet fan of Gully A allowed for a more detailed reconstruction of the erosion history of this specific gully. Most of the material exposed in the profiles was undoubtedly of colluvial origin as evidenced by coarse fragments (shale and pebbles within a matrix of fines), high ^{137}Cs activity at greater depth, embedded artefacts, and plant remnants (Fig. 4; Fig. 5). Prior to soil erosion, the whole study area was covered by Pleistocene loess, on which Mollisols had developed (Fig. 4c). In the profiles at the outlet fan, a clear distinction between the original Mollisol and the black colluvial layer with a high organic content was not always possible in profiles with black bottom layers. However, in many profiles we found clear indications that black sediment derived from the mollic epipedon has been deposited on the fan in the early phase of colluviation. The general sequence of inverted soil profiles is visible in most of the profiles, where the sediments become less dark (i.e. the content of organic carbon decreases) and the content of coarse fragments increases toward the top (Fig. 4).

^{137}Cs-analyses in the profiles P2, P7 and P11 (Fig. 5) allowed for a rough dating of the sediments. The deepest occurrence of ^{137}Cs can be equated with the onset of ^{137}Cs in the 1950s, although a small proportion may have migrated down the profile. High ^{137}Cs concentrations are likely to indicate colluvial sediments from the 1960s, when nuclear fallout reached its maximum (Owens et al., 1997). However, we must consider that the

For Peer Review

initial spatial distribution of ^{137}Cs was not uniform on a large scale (Parsons & Foster, 2011; Zhang, 2015; Zhang et al., 2019a). Furthermore, the ^{137}Cs depth profiles reflect both direct fallout from the atmosphere and delayed input of ^{137}Cs-enriched colluvial sediments from the gully catchment. As the timespan between fallout on the soil surface in the catchment and deposition on the outlet fan is unknown, only rough estimations of the time of deposition can be made.

In profile P1, located in the most distal part of the fan, we found faint structural hints that the original mollic epipedon began at 85 cm depth. The high ^{137}Cs activity between 85 and 95 cm therefore probably reflects direct fallout on the fan. As ^{137}Cs was rapidly absorbed to the fine fraction of the soil and retained in the top few centimeters (Owens et al., 1997), the ^{137}Cs activity dropped sharply in 95-100 cm. The high ^{137}Cs concentrations at 75-85 cm suggest a deposition during the 1960s. The three samples above 75 cm were virtually free from ^{137}Cs and had lighter soil color. These results can be explained by erosion of subsoil material in the gully and subsequent deposition on the fan. The plastic found at 42 cm was recognized as the package of a detergent produced not earlier than 1992. The agricultural plastic foil in profile P2 (60 cm depth) was introduced from Japan not earlier than 1979 (Chen, 2014). These modern artefacts prove that gully erosion continued after large parts of the catchment had been terraced between 1968 and 1974 (Wen et al., 2021).

In profile P7, charcoal, slag, and hard coal particles probably derived from a small brick kiln factory and a small iron boiler established between 1967 and 1970 near the head of the gully. This is in line with high and continuous ^{137}Cs activity between 75 and 130 cm, which can be attributed to the 1960s. Notable ^{137}Cs concentrations could also be detected in most of the samples below down to the lowermost sample in 200-205 cm. It is unlikely that this was caused by post-depositional downward migration in the profile

For Peer Review

because this would create a rather constant decline of ^{137}Cs with increasing depth. The colluvial origin of the whole profile is further indicated by numerous shale fragments and some pebbles in the lowermost sediments (>140 cm depth). This, in turn, suggests that a gully had existed when the sediments were deposited. Otherwise, it would not have been possible to deliver shale and pebbles to the outlet fan. We conclude that the lower part of P7 is a colluvial sediment from the 1950s, while the sediments with higher ^{137}Cs concentrations between ca. 60 and 130 cm were deposited from the 1960s onward. The upper sediments mainly result from erosion of subsoil and shale in the gully.

Profile P11 is located at the most proximal position of the outlet fan and therefore probably received the earliest colluvial deposits. The well-preserved horsetail stems found in the two lowermost layers indicate a young colluvial origin of the whole profile. Considerable amounts of ^{137}Cs were detected between 95 and 130 cm, suggesting a deposition between ca. 1955 and 1970. The pronounced peak at 95-105 cm might be equated with the fallout peaks around 1963. The upper 85 cm of P11 are virtually free from ^{137}Cs. As in P7, these sediments derive from subsoil and shale eroded in the gully.

Thus, Gully A already existed prior to the 1960s. However, until the 1960s, erosion mostly affected the deep mollic surface horizons in the catchment. The outlet deposit fan out of the gully reflects rapid extension and cutting down from then on to the present despite terracing and afforestation in parts of the catchment (Fig. 3d).

4.2. Gully erosion rates and driving forces

The mean gully density in the study area is 2.3 km km^{-2} (Table 1). Gully densities in the same order of magnitude have been observed in other parts of the Mollisol region of Northeast China (Liu et al., 2020; Xu et al., 2014; Yang et al., 2017). A recent case study from the Mollisol region reported that gully density had increased by a factor of 4.3 from

For Peer Review

0.16 km km^{-2} in 1965 to 0.67 km km^{-2} in 2015 (Li et al., 2021). 4.3 km km^{-2} have been reported from the upper reaches of Yangtze River, Southwest China, and 5.9 km km^{-2} from the Loess Plateau, Northwest China (Liu et al., 2013; Xu et al., 2018). The gully head retreat rates of 1.5 to 2.5 m yr^{-1} in our study area (Table 2) are lower than average head retreat rates obtained elsewhere in the Mollisol region of Northeast China (6.2 m yr^{-1}, Hu et al., 2007; 8.4 m yr^{-1}, Wu et al., 2008). However, the soil loss rates from our studied gullies (Table 2) were much higher than previously reported from the Mollisol region of Northeast China (10.1 Mg ha^{-1} yr^{-1}, Wu et al., 2008; 4.5 Mg ha^{-1} yr^{-1}, An et al., 2014). These differences can be explained by the smaller size and younger age of the gullies studied by Wu et al. (2008). Larger and deeper main gullies, soil loss from the side gullies, longer-term sidewall collapsing and downcutting of the gully floor cause a relatively high soil loss from our studied gullies. However, the retreat rates of the main gully head might be rather slow, partly because of the limited drainage areas above the advancing gully heads.

In China, the southwestern and northwestern regions are most famous for gully erosion before the 1990s and for effective soil erosion control after the campaign of "Grain for Green" since the 2000s (Cao et al., 2009; Li et al., 2020; Zhao et al., 2013). The soil loss rates obtained from our study area are as high as those in the Loess Plateau of Northwest China (18.8 to 43.0 Mg ha^{-1} yr^{-1}; Poesen et al., 2003), but lower than in the Dry-hot valley region of Southwest China (164 Mg ha^{-1} yr^{-1}, Yang et al., 2015). Compared to the southwestern and northwestern regions of China, precipitation is lower, slopes are gentler, and soils are richer in organic carbon in the Mollisol region of Northeast China. However, gully extension rates and soil loss rates by gullying are high and terracing and reforestation did not successfully control gully erosion as reported in many other regions of China.

For Peer Review

Apart from the overall impact of arable land use, there are several other environmental conditions that explain the on-going fast development of gullies over the last decades in the study area. Firstly, the soils have a high clay content of about 40% (Sui et al., 2013; Qiao et al., 2015) and are deeply frozen during the long winter. Despite a high content of organic carbon, the soils are very weak in soil structure in May when plants and crops start to grow due to the strong freezing and thawing cycles in winter and early spring (Li & Fan, 2014; Wang et al., 2012; Ma et al., 2019). The soil bulk density can change dramatically from 1.01 Mg m^{-3} (total porosity > 64%) in May to 1.40 Mg m^{-3} in August due to gravity and mechanical compaction during maize cropping (Chen et al., 2014; Jiang et al., 2018). Due to the high clay content, soil water infiltration rate at zero tension was reported to be as low as 25×10^{-6} m s^{-1} in May and August irrespective of the difference in soil bulk density (Jiang et al., 2018). Low infiltration rates cause runoff formation during snowmelt and in the rainy season. During snowmelt, the soils are usually frozen and impermeable beneath 20 cm and therefore become rapidly saturated, which causes a large amount of overland flow, especially when additional water is added by precipitation in spring (Hu et al., 2007; Ma et al., 2019; Xu et al., 2019b). Frequent and intensive freezing and thawing in winter further contributes to the destabilization of gully walls and mass-wasting (Collison, 2001; Hu et al., 2007; Ma et al., 2019; Xu et al., 2019b).

Soil piping contributes to gully development under a wide range of climate conditions (Addisie et al., 2017; Bernatek-Jakiel & Wrońska-Wałach, 2018a; Bernatek-Jakiel & Poesen, 2018b; Verachtert et al., 2010). We found only a few small open holes linked belowground at upper part of slopes during extensive field surveys and mapping campaigns, indicating that piping exists, but is not an important driver of gully development.

For Peer Review

Secondly, the loess-like parent material of the Mollisols is underlain by fluvial deposits with sand and pebble layers of low cohesion and poorly consolidated shales. These shales are highly prone to frost weathering. The weathered shale fragments accumulate at the gully floor before they are washed away. These processes were observed in many gullies located on the steep slopes along the Hailun River plain, e.g. Gully C (Fig. 3b and c). Once these strata are exposed at the gully walls, gully-wall collapse due to gravity accelerates gully widening and may foster the slumping of the mollic surface soil even if plant roots stabilize the soil as shown in the study area (Wen et al., 2021) and other regions (Barnes et al., 2016; Vanmaercke et al., 2016).

Thirdly, field cart roads facilitate the concentration of overland flow, increasing shear stress and scouring force along the roads and accelerating gully development (Fig. 3a). This effect was obvious in the case of Gully C, showing two parallel straight gully segments in its lower section along a road in 2018 (Fig. 3c). The road ran a few meters away from the original gully in 1968 and shifted its position due to incision of the second gully, which was still active in 2018. Gully erosion along unpaved roads has also been reported from China´s Loess Plateau (Zhang et al., 2019b).

Finally, many gullies were still active and even new gullies developed on abandoned and partly afforested slopes due to improper terrace design and a lack of terrace maintenance after reforestation (Wen et al., 2021).

5. Conclusions

This study demonstrated that gully erosion started in the 1950s when the original grasslands and shrub forests were converted into arable land on a large scale in the Mollisol region of Northeast China. Most gully systems initiated on steeper slopes where unconsolidated sediments and cohesionless shales lie close to the surface. Gully

For Peer Review

erosion accelerated during the 1960s and continued up to the present despite afforestation and terracing. The mean gully density doubled from 1.2 km km^{-2} in 1968 to 2.3 km km^{-2} in 2018. Four gullies which have been studied in detail expanded at rates of 1.5 to 2.5 m yr^{-1} between 1968 and 2018, resulting in soil loss at rates of 25.7 to 44.7 Mg ha^{-1} yr^{-1}. The estimated gully erosion rates are comparably as high as, or even higher than, the reported data from many regions around the world well-known for heavy gully erosion. Our findings point out the severeness of gully erosion in the Mollisol region of Northeast China and highlight the need of taking prompt and proper countermeasures to retain surface runoff.

Acknowledgements

This study was funded by the National Key Research and Development Program of China (No. 2017YFC0504202/GX18B028). Xu Jinzhong and Zhen Huaicai helped in field investigations.

Author contributions

Bin ZHANG: Study design; Yanru WEN, Bin ZHANG, Till KASIELKE and Harald ZEPP: Profile sample collection in the field, data interpretation and paper drafting. Yanru WEN and Hao LI: DEM and UAV survey.

References

Aber, J. S., Marzolff, I., Ries, J. B., & Aber, S. E. W. (2019). Gully-Erosion Monitoring. In J. S. Aber, I. Marzolff, J. B. Ries, & S. E. W. Aber (Eds.), *Small-Format Aerial Photography and UAS Imagery* (pp. 259-271). Amsterdam: Elsevier.

For Peer Review

Addisie, M. B., Ayele, G. K., Gessess, A. A., Tilahun, S. A., Zegeye, A. D., Moges, M. M., Schmitter, P., Langendoen, E. J., & Steenhuis, T. S. (2017). Gully Head Retreat in the Sub-Humid Ethiopian Highlands: The Ene-Chilala Catchment. *Land Degradation & Development, 28*(5), 1579-1588. doi:10.1002/ldr.2688

An, J., Zheng, F., & Wang, B. (2014). Using ^{137}Cs technique to investigate the spatial distribution of erosion and deposition regimes for a small catchment in the black soil region, Northeast China. *Catena, 123*, 243-251. doi:10.1016/j.catena.2014.08.009

Barnes, N., Luffman, I., & Nandi, A. (2016). Gully erosion and freeze-thaw processes in clay-rich soils, northeast Tennessee, USA. *GeoResJ, 9-12*, 67-76. doi:10.1016/j.grj.2016.09.001

Bernatek-Jakiel, A., & Wrońska-Wałach, D. (2018a). Impact of piping on gully development in mid-altitude mountains under a temperate climate: A dendrogeomorphological approach. *Catena, 165*, 320-332. doi:10.1016/j.catena.2018.02.012

Bernatek-Jakiel, A., & Poesen, J. (2018b). Subsurface erosion by soil piping: significance and research needs. *Earth-Science Reviews, 185*, 1107-1128. doi:10.1016/j.earscirev.2018.08.006

Bork, H. R., & Lang, A. (2003). Quantification of past soil erosion and land use / land cover changes in Germany. In A. Lang, R. Dikau, & K. Hennrich (Eds.), *Long Term Hillslope and Fluvial System Modelling* (pp. 231-239). Berlin, Heidelberg: Springer.

Cao, S., Chen, L., & Yu, X. (2009). Impact of China's Grain for Green Project on the landscape of vulnerable arid and semi-arid agricultural regions: a case study in

For Peer Review

northern Shaanxi Province. *Journal of Applied Ecology, 46*(3), 536-543. doi:10.1111/j.1365-2664.2008.01605.x

Castillo, C., & Gomez, J. A. (2016). A century of gully erosion research: Urgency, complexity and study approaches. *Earth-Science Reviews, 160*, 300-319. doi:10.1016/j.earscirev.2016.07.009

Chen, D. (2014). Application Status and Development of Mulch Film in China. *Sugarcane and Canesugar,* (4), 50-54 (In Chinese with English abstract).

Chen, X., Liang, A., Jia, S., Zhang, P., & Wei, C. (2014). Impact of tillage on physical characteristics in a Mollisol of Northeast China. *Plant, Soil and Environment, 60*, 309-313. doi:10.17221/245/2014-PSE

Collison, A. J. C. (2001). The cycle of instability: stress release and fissure flow as controls on gully head retreat. *Hydrological Processes, 15*(1), 3-12. doi:10.1002/hyp.150

Dotterweich, M. (2008). The history of soil erosion and fluvial deposits in small catchments of central Europe: Deciphering the long-term interaction between humans and the environment – A review. *Geomorphology, 101*, 192-208. doi:10.1016/j.geomorph.2008.05.023

Dotterweich, M. (2013). The history of human-induced soil erosion: Geomorphic legacies, early descriptions and research, and the development of soil conservation – A global synopsis. *Geomorphology, 201*, 1-34. doi:10.1016/j.geomorph.2013.07.021

Dotterweich, M., Schmitt, A., Schmidtchen, G., & Bork, H. R. (2003). Quantifying historical gully erosion in northern Bavaria. *Catena, 50*(2-4), 135-150. doi:10.1016/S0341-8162(02)00142-X

For Peer Review

Dreibrodt, S., Lubos, C., Terhorst, B., Damm, B., & Bork, H. R. (2010). Historical soil erosion by water in Germany: Scales and archives, chronology, research perspectives. *Quaternary International, 222*(1), 80-95. doi:10.1016/j.quaint.2009.06.014

Fang, H., Sun, L., Qi, L., & Cai, G. (2012). Using ^{137}Cs technique to quantify soil erosion and deposition rates in an agricultural catchment in the black soil region, Northeast China. *Geomorphology, 169-170*, 142-150. doi:10.1016/j.geomorph.2012.04.019

FAO (Food and Agriculture Organization of the United Nations). (2006). Guidelines for soil description. 4th edition. Rome.

FAO (Food and Agriculture Organization of the United Nations). (2015). World reference base for soil resources 2014. International soil classification system for naming soils and creating legends for soil maps. Update 2015. World Soil Resources Reports 106. Rome.

Frankl, A., Nyssen, J., De Dapper, M., Haile, M., Billi, P., Munro, R. N., Deckers, J., & Poesen, J. (2011). Linking long-term gully and river channel dynamics to environmental change using repeat photography (Northern Ethiopia). *Geomorphology, 129*(3-4), 238-251. doi:10.1016/j.geomorph.2011.02.018

Frankl, A., Poesen, J., Deckers, J., Haile, M., & Nyssen, J. (2012). Gully head retreat rates in the semi-arid highlands of Northern Ethiopia. *Geomorphology, 173*, 185-195. doi:10.1016/j.geomorph.2012.06.011

Gudino-Elizondo, N., Biggs, T. W., Castillo, C., Bingner, R. L., Langendoen, E. J., Taniguchi, K. T., Kretzschmar, T., Yuan, Y. P., & Liden, D. (2018). Measuring ephemeral gully erosion rates and topographical thresholds in an urban watershed using unmanned aerial systems and structure from motion photogrammetric

For Peer Review

techniques. *Land Degradation & Development, 29*(6), 1896-1905. doi:10.1002/ldr.2976

Harvey, A. M. (1992). Process interactions, temporal scales and the development of hillslope gully systems: Howgill Fells, northwest England. *Geomorphology, 5*(3-5), 323-344. doi:10.1016/0169-555x(92)90012-d

Hu, G., Wu, Y., Liu, B., Yu, Z. You, Z., & Zhang, Y. (2007). Short-term gully retreat rates over rolling hill areas in black soil of Northeast China. *Catena, 71*(2), 321-329. doi:10.1016/j.catena.2007.02.004

Jiang, H., Han, X., Zou, W., Hao, X., & Zhang, B. (2018). Seasonal and long-term changes in soil physical properties and organic carbon fractions as affected by manure application rates in the Mollisol region of Northeast China. *Agriculture, Ecosystems & Environment, 268*, 133-143. doi:10.1016/j.agee.2018.09.007

Kappler, C., Kaiser, K., Tanski, P., Klos, F., Fulling, A., Mrotzek, A., Sommer, M., & Bens, O. (2018). Stratigraphy and age of colluvial deposits indicating Late Holocene soil erosion in northeastern Germany. *Catena, 170*, 224-245. doi:10.1016/j.catena.2018.06.010

Kasielke, T., Poch, R. M., & Wiedner, K. (2019). Chernozem relics in the Hellweg Loess Belt (Westphalia, NW Germany) - Natural or man-made? *Quaternary International, 502*, 296-308. doi:10.1016/j.quaint.2018.09.015

Kasielke, T., & Zepp, H. (2011). Sediment fillings in valleys of the Ruhr area resulting from human impact in different periods of history. *Zeitschrift Fur Geomorphologie, 55*, 51-65. doi:10.1127/0372-8854/2011/0055s1-0037

Kosov, B. F., Nikol'skaya, I. I. & Zorina, YE. F. (1978). Eksperimental'nyye issledovaniya ovragoobrazovaniya. In: N.I. Makkaveev, Eksperimental'naya geomorfologiya, v.3, Izd. Mosk. Univ., Moskva, pp 113-140. (In Russian)

For Peer Review

Li, H., Cruse, R.M., Liu, X., & Zhang, X. (2016). Effects of topography and land use change on gully development in typical mollisol region of Northeast China. *Chinese Geographical Science. 26* (6), 779-788. doi:10.1007/s11769-016-0837-7.

Li, G., & Fan, H. (2014). Effect of Freeze-Thaw on Water Stability of Aggregates in a Black Soil of Northeast China. *Pedosphere, 24*(2), 285-290 (In Chinese with English abstract).

Li, M., Li, T., Zhu, L., Meadows, M., Zhu, W., & Zhang, S. (2021). Effect of Land Use Change on Gully Erosion Density in the Black Soil Region of Northeast China From 1965 to 2015: A Case Study of the Kedong County, *Frontiers in Environmental Science,* 9, 652933. doi: 10.3389/fenvs.2021.652933

Li, Z., Ning, K., Chen, J., Liu, C., Wang, D., Nie, X., Hu, X., Wang, L., & Wang, T. (2020). Soil and water conservation effects driven by the implementation of ecological restoration projects: Evidence from the red soil hilly region of China in the last three decades. *Journal of Cleaner Production, 260*, 13. doi:10.1016/j.jclepro.2020.121109

Liu, L., Chen, S., Sun, J., & Zhao, T. (2013). Analysis on the watershed features in hilly and gulliy loess area in west Shanxi. *Journal of Arid Land Resources & Environment, 27*(4), 146-152 (In Chinese with English abstract).

Liu, S., Cui, B., Zhang, Y., & Yang, X. (2020). Effects of topographical factors on erosion gully distribution of farmland in hilly areas of Jinlin Province. *Bulletin of Soil and Water Conservation, 40*(1), 38-42 (In Chinese with English abstract).

Liu, X., Burras, C. L., Kravchenko, Y. S., Duran, A., Huffman, T., Morras, H., Studdert, G., Zhang, X., Cruse, R. M., & Yuan, X. (2012). Overview of Mollisols in the world: Distribution, land use and management. *Canadian Journal of Soil Science, 92*(3), 383-402. doi:10.4141/Cjss2010-058

For Peer Review

Liu, X., & Yan, B. (2009). Soil loss and food safety in Northeast China. Soil and Water Conservation in China. *Soil and Water Conservation in China*, (1), 17-19 (In Chinese with English abstract).

Liu, X., Zhang, S., Zhang, X., Ding, G., & Cruse, R. M. (2011). Soil erosion control practices in Northeast China: A mini-review. *Soil & Tillage Research, 117*, 44-48. doi:10.1016/j.still.2011.08.005

Ma, Q., Zhang, K., Jabro, J. D., Ren, L., & Liu, H. (2019). Freeze–thaw cycles effects on soil physical properties under different degraded conditions in Northeast China. *Environmental Earth Sciences, 78*(10), 12. doi:10.1007/s12665-019-8323-z

Marzolff, I., & Poesen, J. (2009). The potential of 3D gully monitoring with GIS using high-resolution aerial photography and a digital photogrammetry system. *Geomorphology, 111*(1-2), 48-60. doi:10.1016/j.geomorph.2008.05.047

Mieth, A., & Bork, H. R. (2010). Humans, climate or introduced rats – which is to blame for the woodland destruction on prehistoric Rapa Nui (Easter Island)? *Journal of Archaeological Science, 37*(2), 417-426. doi:10.1016/j.jas.2009.10.006

Ministry of Water Resources, Chinese Academy of Sciences, & Engineering., C. A. O. (2010). *Soil erosion prevention and ecological security in China: The Black Soil Region in Northeast China*. Beijing: Science Press (In Chinese).

Moges, A., & Holden, N. M. (2008). Estimating the rate and consequences of gully development, a case study of Umbulo catchment in Southern Ethiopia. *Land Degradation & Development, 19*(5), 574-586. doi:10.1002/ldr.871

Nyssen, J., Poesen, J., Veyret-Picot, M., Moeyersons, J., Haile, M., Deckers, J., Dewit, J., Naudts, J., Teka, K., & Govers, G. (2006). Assessment of gully erosion rates through interviews and measurements: a case study from northern Ethiopia. *Earth Surface Processes and Landforms, 31*(2), 167-185. doi:10.1002/esp.1317

For Peer Review

Owens, P. N., Walling, D. E., He, Q. P., Shanahan, J., & Foster, I. D. L. (1997). The use of caesium-137 measurements to establish a sediment budget for the Start catchment, Devon, UK. *Hydrological Sciences Journal, 42*(3), 405-423. doi:10.1080/02626669709492037

Parsons, A. J., & Foster, I. D. L. (2011). What can we learn about soil erosion from the use of ^{137}Cs? *Earth-Science Reviews, 108*(1-2), 101-113. doi:10.1016/j.earscirev.2011.06.004

Poesen, J. (2018). Soil erosion in the Anthropocene: Research needs. *Earth Surface Processes and Landforms, 43*(1), 64-84. doi:10.1002/esp.4250

Poesen, J., Nachtergaele, J., Verstraeten, G., & Valentin, C. (2003). Gully erosion and environmental change: importance and research needs. *Catena, 50*(2-4), 91-133. doi:10.1016/S0341-8162(02)00143-1

Porto, P., & Walling, D. E. (2012). Validating the use of ^{137}Cs and ^{210}Pb$_{ex}$ measurements to estimate rates of soil loss from cultivated land in southern Italy. *Journal of Environmental Radioactivity, 106*, 47-57. doi:10.1016/j.jenvrad.2011.11.005

Qiao, Y., Miao, S., Na, L., Xu, Y., Han, X., & Zhang, B. (2015). Crop species affect soil organic carbon turnover in soil profile and among aggregate sizes in a Mollisol as estimated from natural ^{13}C abundance. *Plant and Soil, 392*, 163-172. doi:10.1007/s11104-015-2414-8

Soil Survey Staff. (2010). *Keys to soil taxonomy*. United States Department of Agriculture, Washington, D.C.: Government Printing Office.

Sui, Y., Liu, G., Gu, S., Zhang, X., & Meng, K. (2005). Investigation of the black soil physical and chemical properties in Northeast China. *System Sciences and*

For Peer Review

Comprehensive Studies in Agriculture, 21(4), 290-301. (In Chinese with English abstract).

Sui, Y., Jiao, X., Chen, W., Liu, X., Zhang, X., & Ding, G. (2013). Labile Organic Matter Content and Distribution as Affected by Six-year Soil Amendments to Eroded Chinese Mollisols. *Chinese Geographical Science, 2*3(6), 692-699. doi:10.1007/s11769-013-0639-0

Sun, J., & Liu, T. (2001). Desertification in the Northeastern China. *Quaternary Sciences, 21*(1), 72-78 (In Chinese with English abstract).

Sutherland, R. A. (1989). Quantification of accelerated soil erosion using the environmental tracer caesium-137. *Land Degradation and Development, 1*(3), 199-208. doi:10.1002/ldr.3400010304

Tebebu, T. Y., Abiy, A. Z., Zegeye, A. D., Dahlke, H. E., Easton, Z. M., Tilahun, S. A., Collick, A. S., Kidnau, S., Moges, S., Dadgari, F., & Steenhuis, T. S. (2010). Surface and subsurface flow effect on permanent gully formation and upland erosion near Lake Tana in the northern highlands of Ethiopia. *Hydrology and Earth System Sciences, 14*(11), 2207-2217. doi:10.5194/hess-14-2207-2010

Vandekerckhove, L., Poesen, J., Wijdenes, D. O., & Gyssels, G. (2001). Short-term bank gully retreat rates in Mediterranean environments. *Catena, 44*(2), 133-161. doi:10.1016/S0341-8162(00)00152-1

Vanmaercke, M., Poesen, J., Van Mele, B., Demuzere, M., Bruynseels, A., Golosov, V., Bezerra, J. F. R., Bolysov, S., Dvinskih, A., Frankl, A., Fuseina, Y., Guerra, A. J. T., Haregeweyn, N., Ionita, I., Makanzu Imwangana, F., Moeyersons, J., Moshe, I., Nazari Samani, A., Niacsu, L., Nyssen, J., Otsuki, Y., Radoane, M., Rysin, I., Ryzhov, Y. V., & Yermolaev, O. (2016). How fast do gully headcuts

For Peer Review

retreat? *Earth-Science Reviews, 154*, 336-355. doi:10.1016/j.earscirev.2016.01.009

Vattuone, M. S., Monne, J. L. P., Roldan, J., Maldonado, M., Lefebvre, M., & Vattuone, M. (2018). Human-driven geomorphological processes and soil degradation in Northwest Argentina: A geoarchaeological view. *Land Degradation & Development, 29*(11), 3852-3865. doi:10.1002/ldr.3128

Verachtert, E., Van den Eeckhaut, M., Poesen, J., & Deckers, J. (2010). Factors controlling the spatial distribution of soil piping erosion on loess-derived soils: A case study from central Belgium. *Geomorphology, 118*(3-4), 339-348. doi:10.1016/j.geomorph.2010.02.001

Walling, D. E., & Quine, T. A. (1990). Calibration of caesium-137 measurements to provide quantitative erosion rate data. *Land Degradation and Development, 2*(3), 161-175. doi:10.1002/ldr.3400020302

Wang, E., Cruse, R. M., Chen, X., & Daigh, A. (2012). Effects of moisture condition and freeze/thaw cycles on surface soil aggregate size distribution and stability. *Canadian Journal of Soil Science, 92*(3), 529-536. doi:10.4141/cjss2010-044

Wen, Y., Kasielke, T., Li, H., Zhang, B., & Zepp, H. (2021). May agricultural terraces induce gully erosion? A case study from the Black Soil Region of Northeast China. *Science of the Total Environment, 750*, 141715. doi:10.1016/j.scitotenv.2020.141715

Wilson, G. V., Rigby, J. R., & Dabney, S. M. (2015). Soil pipe collapses in a loess pasture of Goodwin Creek watershed, Mississippi: role of soil properties and past land use. *Earth Surface Processes and Landforms, 40*(11), 1448-1463. doi:10.1002/esp.3727

For Peer Review

Wu, Y., Zheng, Q., Zhang, Y., Liu, B., Cheng, H., & Wang, Y. (2008). Development of gullies and sediment production in the black soil region of northeastern China. *Geomorphology, 101*(4), 683-691. doi:10.1016/j.geomorph.2008.03.008

Xu, Q., Kou, P., Wang, C., Yunus, A., Xu, J., Peng, S., & He, C. (2019a). Evaluation of gully head retreat and fill rates based on high-resolution satellite images in the loess region of China. *Environmental Earth Sciences, 78*, 465. doi:10.1007/s12665-019-8483-x

Xu, J.., Li, H., Liu, X., Hu, W., Yang, Q., Hao, Y., Zhen, H., & Zhang, X. (2019b). Gully erosion induced by snowmelt in northeast china: A case study. *Sustainability, 11*(7), 2088. doi:10.3390/su11072088

Xu, X., Sui, Y., & Zhang, Y. (2014). Development of gully erosion and its influencing factors in hilly regions of Northeast China. *Acta Pedologica Sinica, 4*, 699-708 (In Chinese with English abstract).

Xu, Z., Qin, F., Zhang, B., Deng, Q., Liu, H., Jin, J., & Shi, L. (2018). The morphological characteristics of gully systems and watersheds in Dry-Hot Valley, SW China. *Acta Geochimica, 37*(6), 854-866. doi:10.1007/s11631-018-0299-y

Yang, D., Xiong, D., Guo, M., Su, Z., Zhang, B., Zheng, X. Zhang, S., & Fang, H. (2015). Impact of grass belt position on the hydraulic properties of runoff in gully beds in the Yuanmou Dry-hot valley region of Southwest China. *Physical Geography, 36*(5), 408-425. doi:10.1080/02723646.2015.1074517

Yang, J., Zhang, S., Chang, L., Li, F., Li, T., & Gao, Y. (2017). Gully erosion regionalization of black soil area in northeastern China. *Chinese Geographical Science, 27*(1), 78-87. doi:10.1007/s11769-017-0848-z

For Peer Review

Ye, Y., & Fang, X. (2011). Spatial pattern of land cover changes across Northeast China over the past 300 years. *Journal of Historical Geography, 37*(4), 408-417. doi:10.1016/j.jhg.2011.08.018

Zhang, X., Polyakov, O., Liu, B., & Nearing, A. (2019). Quantifying geostatistical properties of ^{137}Cs and $^{210}Pb_{ex}$ at small scales for improving sampling design and soil erosion estimation. *Geoderma, 334*, 155-164. doi:10.1016/j.geoderma.2018.08.002

Zhang, X. (2015). New insights on using fallout radionuclides to estimate soil redistribution rates. *Soil Science Society of America Journal, 79*(1), 1-8. doi:10.2136/sssaj2014.06.0261

Zhang, Y., Zhao, Y., Liu, B., Wang, Z., & Zhang, S. (2019). Rill and gully erosion on unpaved roads under heavy rainfall in agricultural watersheds on China's Loess Plateau. *Agriculture, Ecosystems & Environment, 284*, 106580. doi:10.1016/j.agee.2019.106580

Zhang, Y., Wu, Y., Lin, B., Zheng, Q., & Yin, J. (2007). Characteristics and factors controlling the development of ephemeral gullies in cultivated catchments of black soil region, Northeast China. *Soil & Tillage Research, 96*(1-2), 28-41. doi:10.1016/j.still.2007.02.010

Zhang, Y., Long, Y., Li, B., Xu, S. Wang, X., & Liao, J. (2017). Use of reservoir deposits to reconstruct the recent changes in sediment yields from a small granite catchment in the Yimeng Mountain region, China. *Geomorphology, 293*, 167-177. doi:10.1016/j.geomorph.2017.05.017

Zhao, G., Mu, X., Wen, Z., Wang, F., & Gao, P. (2013). Soil erosion, conservation, and eco-environment changes in the Loess Plateau of China. *Land Degradation & Development, 24*(5), 499-510. doi:10.1002/ldr.2246

For Peer Review

Zhu, T. (2012). Gully and tunnel erosion in the hilly Loess Plateau region, China. *Geomorphology, 153*, 144-155. doi:10.1016/j.geomorph.2012.02.019

Figure Captions

Figure 1. Location of the study area in the Mollisol region of Northeast China (a). Gully distribution in the study area in 1968 (b) and 2018 (c). Gullies A-D used to measure gully volume in 2018 are marked.

Figure 2. Morphological changes of Gullies A-D between 1968 and 2018.

Figure 3. Exemplification of gully development processes in the study area. (a) Gully head retreat along a field cart road, (b) downcutting in weathered shales, (c) two parallel segments of Gully C incised along former field cart roads, (d) sidewall expansion and side gully development in Gully A.

Figure 4. Sketched soil profiles along a trench (a) and their positions at the outlet fan of Gully A (b), in comparison to a typical soil profile that was not affected by gully erosion (c). The colors were filled to resemble those of fresh soils.

Figure 5. Distribution of ^{137}Cs in Bq kg^{-1} in selected soil profiles at the outlet fan of Gully A shown in Fig. 4 and at the reference site. ^{137}Cs-samples are marked with an asterisk (*) to show zero values. A complete legend is shown in Fig. 4.

Supplementary

Figure S1. Orthophoto of the studied Gullies A–D captured by the UAV. Ground control and check point locations are marked.

Table S1. Processing and camera self-calibration results from the measurements at Gullies A–D in April 2018 using structure-from-motion with multi-view stereo

For Peer Review

photogrammetry and photos taken by an unmanned aerial vehicle. Px, Py are the [x, y] principal points, R1, R2, R3 are radial distortion coefficients, T1, T2 are tangential distortion coefficients. GCP = ground control point; RMSE = root-mean-square error.

For Peer Review

Table 1. Catchment areas and lengths of total, main and active gullies, gully density and forest land proportion within 20 gully catchments of the study area in 2018 compared to the total gully length in 1968.

Catchment No.	Catchment area (km^2)	Total gully length in 1968 (km)	Length in 2018 (km)					Gully density in 2018 (km km^{-2})	Forest land in 2018† (%)
			Total gullies	Main gully	Active gullies	Total gullies in forest land	Active gullies in forest land		
1	0.91	2.1	3.8	1	3.3	3.2	2.9	4.2	22
2	0.11	0.4	0.3	0.1	0.3	0.3	0.3	2.7	55
3	0.40	1.2	2.4	0.5	2.1	1.5	1.5	6.0	22
4	0.99	2.4	1.1	0.4	0.8	1.0	0.7	1.1	55
5	0.06	0.0	0.2	0.1	0.2	0.2	0.2	3.3	69
6	0.25	0.2	0.9	0.3	0.8	0.0	0.0	3.6	19
7	1.18	2.0	3.2	1.4	3.2	2.0	2.0	2.7	18
8	0.51	0.3	1.1	0.2	0.9	0.7	0.5	2.2	15
9	0.21	0.1	0.6	0.2	0.6	0.0	0.0	2.9	5
10	1.89	1.6	4.6	1.6	3.2	2.5	1.5	2.4	12
11	0.26	0.3	0.6	0.4	0.5	0.1	0.0	2.3	18
12	0.29	0.0	1.2	0.3	1.1	0.8	0.8	4.1	27
13	2.65	6.9	9.8	2.3	9.0	5.4	4.8	3.7	7
14	1.02	0.2	0.9	0.3	0.7	0.0	0.0	0.9	0
15	0.98	0.9	1.4	0.3	1.4	0.0	0.0	1.4	10
16	1.18	0.9	3.8	1.6	3.8	3.0	3.	3.2	6
17	0.83	1.0	1.7	0.6	1.5	1.1	0.5	2.0	5
18	0.57	0.0	1.5	0.6	0.8	1.7	0.6	2.6	4
19	1.76	1.0	2.7	1.7	2.7	0,0	0.0	1.5	0
20	4.01	2.5	4.9	2.5	4.9	0.0	0.0	1.2	0
Study area	20.06	24.0	46.7	16.4	41.8	23.5	19.3	2.3	11

†, estimated based on visual mapping by canopy cover > 10% and tree heights > 5 m and checked via field surveys.

For Peer Review

Table 2. Initiation years and erosion rates of Gullies A-D estimated from gully length, area and volume changes between 1968 and 2018.

Gullies	Gully initiation year§	Gully length (m)		Gully area (m^2)		Gully drainage area in 2018† (ha)	Gully volume in 2018† (m^3)	Gully soil loss ‡ (Mg)	Gully head retreat distance (m)	Gully head retreat rate (m yr^{-1})	Gully area extension rate (m^2 yr^{-1})	Gully soil loss rate¶ (m^3 yr^{-1})	Gully soil loss rate per drainage area (m^3 ha^{-1} yr^{-1})
		1968§	2018†	1968§	2018†								
A	~1955 (1950s)	379	547	22724	30962	43.9	93780	119101	155	2.5	165	1861	42.4
B	~1965 (1960s)	64	246	295	6726	12.7	17045	21647	111	2.1	129	401	31.6
C	~1966 (1960s)	87	300	186	5223	5.4	10070	12789	117	2.3	101	241	44.7
D	~1960 (1960s)	98	217	449.6	3273	6.4	7630	9690	85	1.5	57	164	25.7

§, calculated by Eq. 2 (approx. time reported by the farmers).

†, based on DSM in 2018.

‡, calculated by gully volume and average soil bulk density of 1.27 Mg m^{-3} in 2018.

¶, gully volume divided the number of years since gully initiation.

For Peer Review

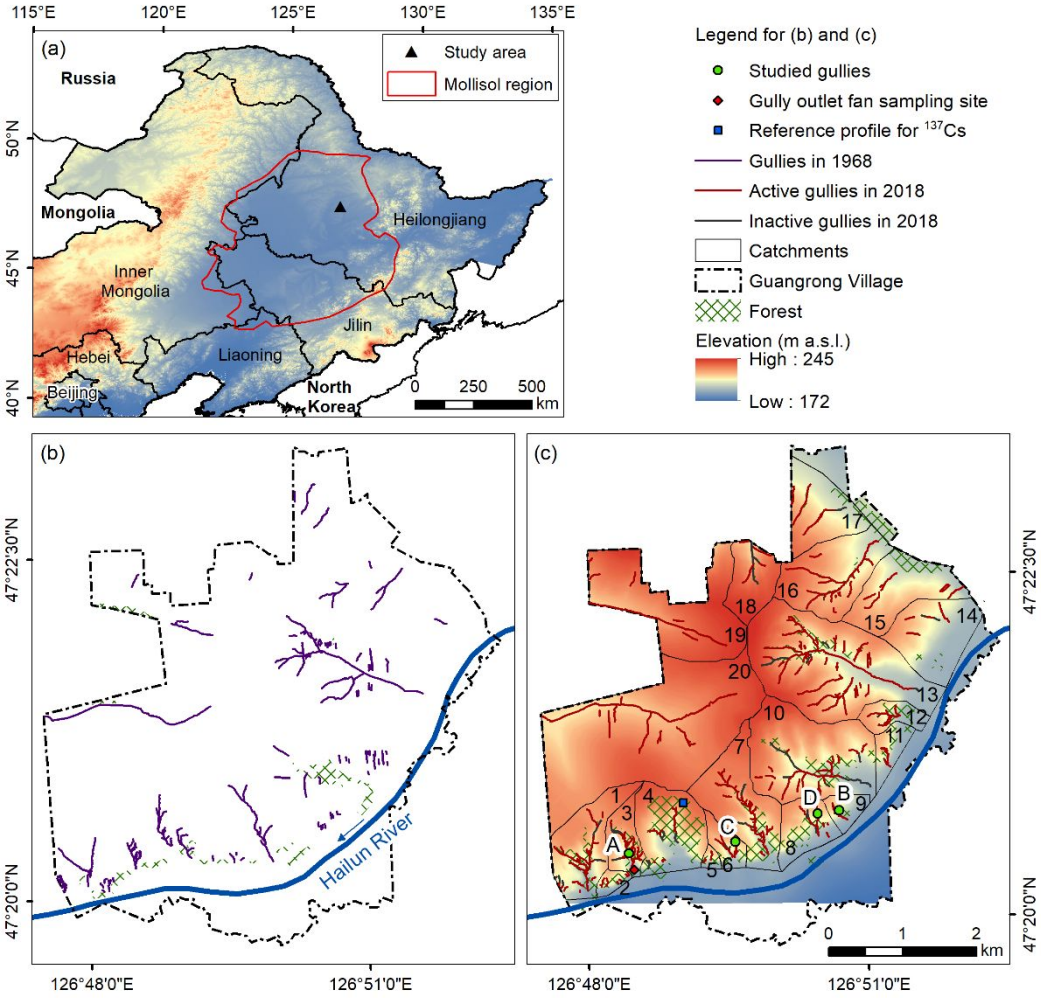

Fig. 1. Location of the study area in the Mollisol region of Northeast China (a). Gully distribution in the study area in 1968 (b) and 2018 (c). Gullies A-D used to measure gully volume in 2018 are marked.

For Review

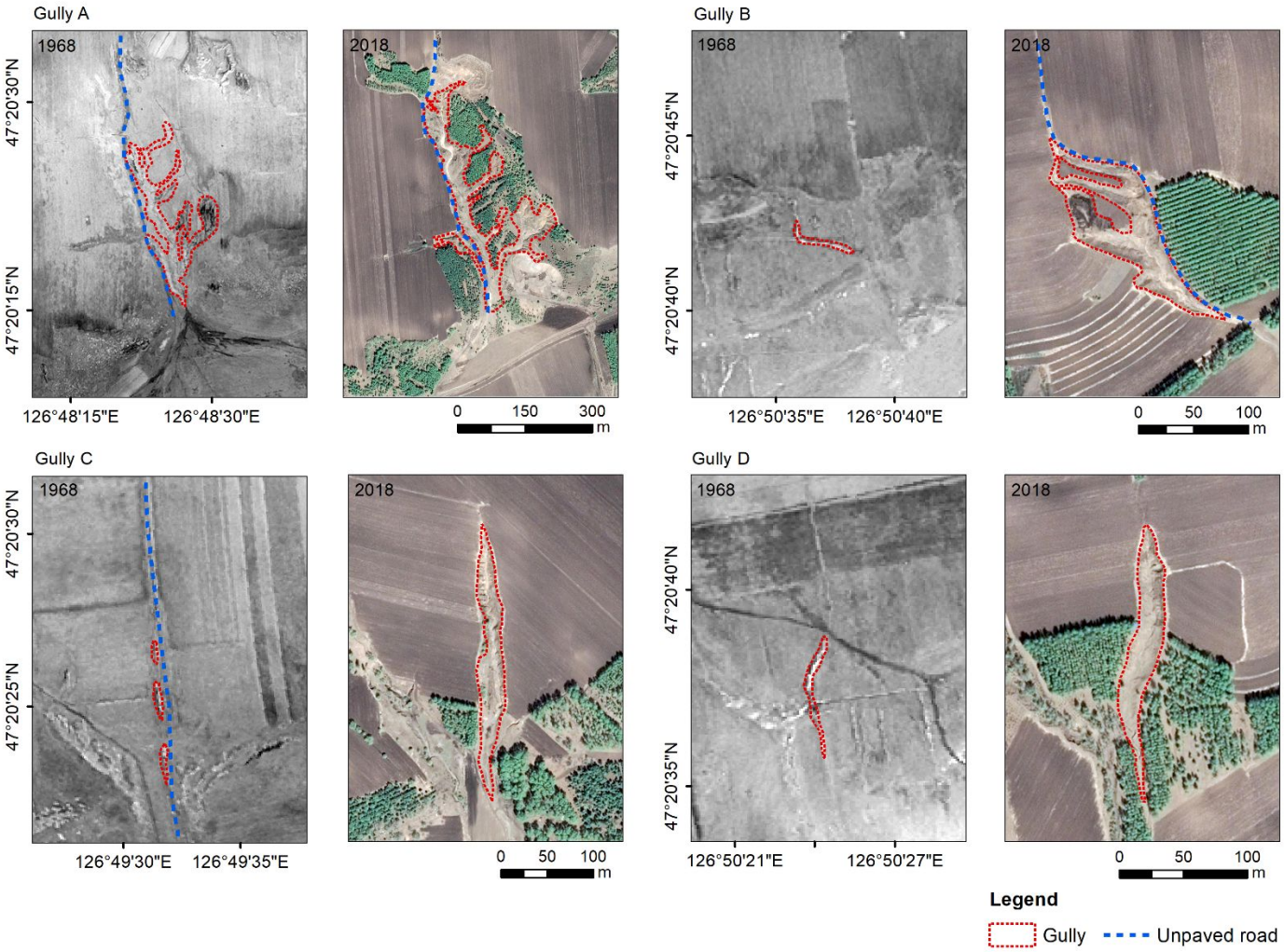

Fig. 2. Morphological changes of Gullies A-D between 1968 and 2018.

7

Fig. 3. Exemplification of gully development processes in the study area. (a) Gully head retreat along a field cart road, (b) downcutting in weathered shales, (c) two parallel segments of Gully C incised along former field cart roads, (d) sidewall expansion and side gully development in Gully A.

For Peer Review

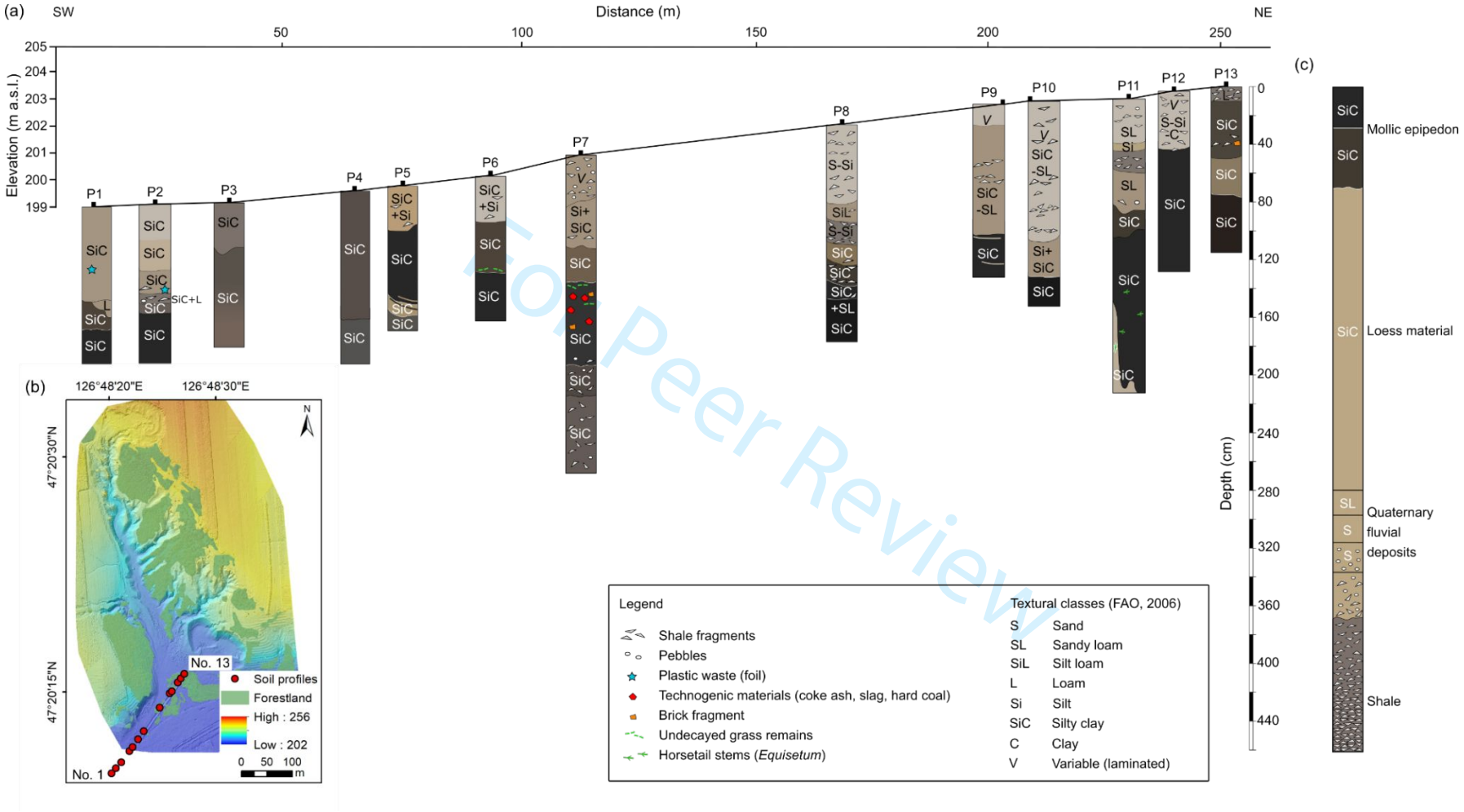

For Peer Review

Fig. 4. Sketched soil profiles along a trench (a) and their positions at the outlet fan of Gully A (b) in comparison to a typical soil profile that was not affected by gully erosion (c). The colors were filled to resemble those of fresh soils.

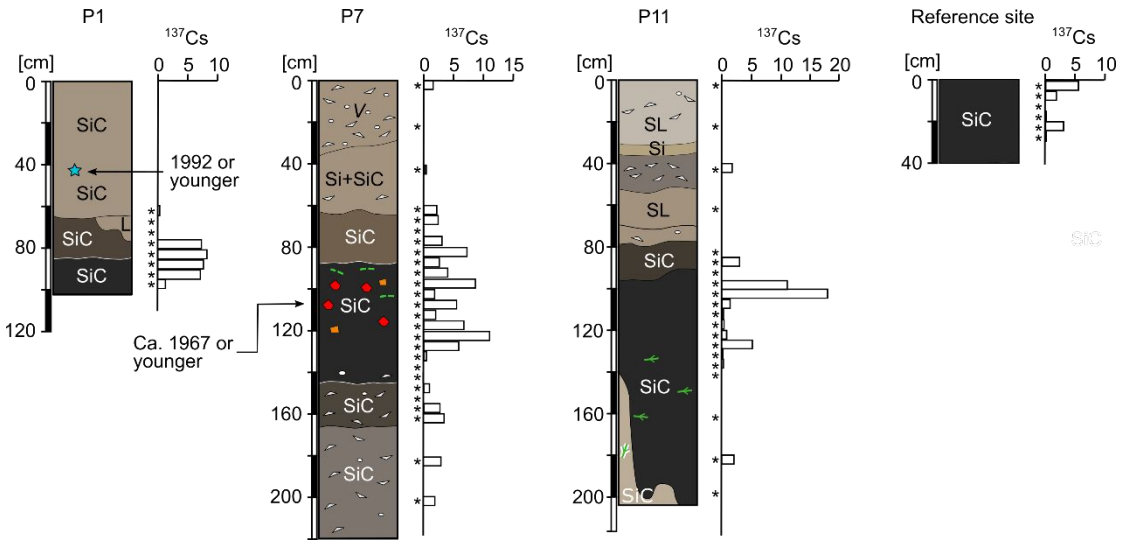

Fig. 5. Distribution of ^{137}Cs in Bq kg^{-1} in selected soil profiles at the outlet fan of Gully A shown in Fig. 4 and at the reference site. ^{137}Cs-samples are marked with an asterisk (*) to show zero values. A complete legend is shown in Fig. 4.

For Peer Review